

INTERNATIONAL SOCIETY FOR SOIL MECHANICS AND GEOTECHNICAL ENGINEERING



This paper was downloaded from the Online Library of the International Society for Soil Mechanics and Geotechnical Engineering (ISSMGE). The library is available here:

<https://www.issmge.org/publications/online-library>

This is an open-access database that archives thousands of papers published under the Auspices of the ISSMGE and maintained by the Innovation and Development Committee of ISSMGE.

PRENOLIN Project: a Benchmark on Numerical Simulation of 1D Non-linear Site Effects. 2 - Results of the Validation Phase

J. Régnier¹, L.F. Bonilla², P.Y. Bard³, H. Kawase⁴, E. Bertrand⁵, F. Hollender⁶, M. Marot⁷, D. Sicilia⁸ and A. Nozu⁹

ABSTRACT

One of the objectives of the PRENOLIN project is the assessment of uncertainties associated with non-linear simulation of 1D site effects. An international benchmark is underway to test several numerical codes, including various non-linear soil constitutive models, to compute the non-linear seismic site response. The preliminary verification phase (i.e. comparison between numerical codes on simple, idealistic cases) is now followed by the validation phase, which compares predictions of such numerical estimations with actual strong motion data recorded from well-known sites. The benchmark presently involves 21 teams and 21 different non-linear computations. Extensive site characterization was performed at three sites of the Japanese KiK-net and PARI networks. The first results indicate that the linear site response is overestimated while the non-linear effects are underestimated. At the end of this phase, most of the epistemic uncertainty sources for non-linear site response analysis is quantified as originating from the constitutive model to the interpretation of the soil data. PRENOLIN is part of two larger projects: SINAPS@, funded by the ANR (French National Research Agency) and SIGMA, funded by a consortium of nuclear operators (EDF, CEA, AREVA, ENL).

Introduction

While a consensus has undoubtedly been reached on the existence of non-linear effects, their quantification and modeling remains a challenge, despite the existence of a commonly accepted practice. The ability to accurately predict non-linear site responses has indeed already been the subject of two recent comparative tests. It was one of the targets of the pioneering blind tests initiated in the late 80's/early 90's on 2 sites of Ashigara Valley (Japan) and Turkey Flat (California); however, those sites lacked strong motion records until the 2004 Parkfield earthquake during which the Turkey Flat site experienced a 0.3g motion. A new benchmarking of 1D non-linear codes was thus carried out in the last decade. Its main findings were reported by Kwok et al., (2008) and Stewart and Kwok, 2009, who emphasized the key importance of the way these codes are used and of the required in-situ measurements. Tests on 2D NL modeling were also attempted within the framework of the Cashima/E2VP project (Bard et al 2011), but

¹Régnier Julie, CEREMA, Nice, France, Julie.regnier@cerema.fr

²Bonilla Luis-Fabian, IFSTTAR, Paris, France, fabian.bonilla@ifsttar.fr

³Bard Pierre-Yves, IFSTTAR / Univ. Grenoble Alpes, ISTERre, Grenoble, France, pierre-yves.bard@ujf-grenoble.fr

⁴Kawase Hirosho, DPRI, Kyoto, Japan, kawase.hiroshi.6x@kyoto-u.ac.jp

⁵Bertrand Etienne, CEREMA, Nice, France, etienne.bertrand@cerema.fr

⁶Hollender Fabrice, CEA, Cadarache, France, fabrice.hollender@cea.fr

⁷Marot Marianne, CEREMA, Nice, France, marianne.marot@hotmail.com

⁸Sicilia Deborah, EDF, Aix-en-Provence, France, deborah.sicilia@edf.fr

⁹Nozu Atsushi, PARI, Yokosuka City, Japan, nozu@pari.go.jp

the coupling of geometrical complexity and non-linearity proved to be premature to perform such kind of computations.

For this reason, the PRENOLIN project considers only 1D soil columns, to test the non-linear codes in the simplest possible, though realistic, geometries. It is organized in two phases: (1) the initial verification phase, aiming at a cross-code comparison on very simple idealistic 1D soil columns with prescribed linear and non-linear parameters; (2) the subsequent, still ongoing validation phase, comparing numerical predictions with actual observations. The target sites are as close as possible to a 1D soil geometry (horizontal stratification), without liquefaction and associated with available sets of downhole and surface recordings for weak and very strong motions. Such pre-existing information has been complemented with careful in-situ and laboratory measurements designed as close as possible to the team requirements. The sites were selected within the Japanese KiK-net and PARI (Port and Airport Research Institute) networks.

In this article, we present the results of the first iteration of the validation phase, which consisted in forward computations without knowledge of the true surface soil response, while in the following iterations, this information was made available to the participating teams.

The Codes Tested

We compared 21 different numerical codes used by 21 participating teams; some teams tested several codes and some codes were tested by different teams: SeismoSoil (A-0), FLIP (B-0), PSNL (C-0), CYBERQUAKE (D-0), NOAH-2D (E-0), DEEPSOIL (J-0 equivalent linear method and J-1, F-0 and M-2, for the non-linear method) NL-DYAS (G-0), OPENSEES (H-0), 1DFD-NL-IM (K-0), ICFEP (L-1), FLAC.7.00 (M-0), DMOD2000 (M-1), GEFDYN (N-0), EPISPEC1D (Q-0), real ESSI (R-0), ASTER (S-0), SCOSSA-1,2 (T-0), SWAP-3C (U-0), GDNL (Y-0), SANISAND (W-0), EERA (Z-0) and PLAXIS (Z-1).

Site Selection

Sites were selected from the KiK-net and PARI networks. The vertical accelerometric sensor array configuration sensor allowed the calculation of borehole site responses. The PARI sites are much more superficial than the KiK-net sites, the downhole sensor is only ~10 to 15 m deep, and a V_s profile is therefore available down to that depth.

More than 46,000 (six-component) recordings from KiK-net were analyzed, to derive a) the empirical site response at the 688 sites and b) the numerical linear site response from the available V_s profile. Two additional sites from the PARI network were analyzed, Sendai and Onahama (30 and 80 earthquake recordings, respectively).

The site selection was performed on the basis of the following requirements: (1) availability of both strong and weak events recordings, (2) plausibility of a 1D geometrical soil configuration, i.e., satisfactory agreement between numerical and empirical site responses in the linear / weak motion range, and (3) the downhole sensor must not be too deep (depth < 250 m).

To fulfill the first and second criteria, we selected sites that recorded at least two earthquakes with PGAs higher than 50 cm/s^2 at the downhole sensor and we selected 1D KiK-net site

configurations identified and reported by and Thompson et al., (2012), in addition to visual inspections of the comparison between the numerical and empirical site response curves. Initially, 5 KiK-net sites (FKSH14, IBRH13, IWTH04, KSRH10 and NIGH13) and 2 PARI sites were selected, and finally 4 KiK-net sites were removed due to liquefaction susceptibility (FKSH14), rocky geology (IBRH13), mountainous environment (IWTH04) and insufficient nonlinearity (NIGH13). We selected 3 sites among the remaining ones -KSRH10, Onahama and Sendai - to be fully characterized for the purpose of the validation phase.

Site Characterization and Soil Column Definition

An extensive measurement campaign was carried out at each of these 3 sites, to obtain the in-situ V_s , V_p and density profiles (using suspension logging for KSRH10 and downhole PS logging for Onahama and Sendai). Additional MASW measurements were performed to check the spatial variability of the soil properties. To constrain the non-linear soil parameters, multiple laboratory measurements were conducted on (1) Disturbed soil samples: Moisture content, soil particle density, particle size distribution, liquid and plastic limits and (2) Undisturbed soil samples: Wet density, tri-axial compression test (either drained for sandy soil or un-drained for clayey soil), consolidation tests, cyclic undrained tri-axial test for sandy samples and cyclic tri-axial test to obtain the non-linear soil properties. The number and location of the undisturbed soil samples is specified in Table 1, along with the downhole sensor depth, the maximal depth of impedance contrast and the type of soil.

Table 1: Geological characteristics of the 3 selected sites with locations of the undisturbed soil samples.

| Site | Downhole sensor depth (m) | Max. impedance contrast depth (m) | Type of soil | Number of cyclic tri-axial test (location) |
|---------|---------------------------|-----------------------------------|--------------|--|
| Sendai | 8 | 7 | Sand | 2 (3.3 & 5.4 m) |
| Onahama | 11 | 17 | Sand | 3 (4.5, 7.5 & 11.4 m) |
| KSRH10 | 250 | 44 | Sand /clay | 6 (3.5, 7.5, 14.5, 22.5, 29,7 & 34 m) |

These data, together with the observed linear empirical site response, were used by the organizing team to define a soil column to be used by all participants in the first iteration of the validation phase. At the Onahama site, it turned out that the distance between the location of the accelerometric sensors and the complementary drillings was too large compared to the strong spatial variability of the shallow soil parameters. Therefore, the validation phase was continued on Sendai and KSRH10 sites only for the first iteration. The soil column used for these two sites is described in Table 3, and the shear modulus degradation and damping curves with respect to deformation, constructed from the cyclic tri-axial compression test results, are illustrated in Figure 2. The Eq 1 describes the V_s profile at Sendai and V_p is deduced from the Poisson ratio (ν) and V_s values.

$$V_s = V_{s_1} + (V_{s_2} - V_{s_1}) \left[\frac{Z - Z_1}{Z_2 - Z_1} \right]^\alpha, \text{ where } V_{s_1} = 140 \text{ m/s}, V_{s_2} = 460 \text{ m/s}, \alpha = 0.7 \quad (\text{Eq1})$$

Table 2: Soil properties from the Sendai and KSRH10 sites.

| Name | Elastic properties | | | | | | | | NL properties | | | | |
|--------|--------------------|--------|----------|----------|-------|-----------------------------|-----------------|---------------------------------|---------------|----------|-------------|-------|------------------|
| | Layer | Z (m) | Vs (m/s) | Vp (m/s) | ν | ρ (kg/m ³) | Q visco-elastic | ε_{min} elastic (%) | G/Gmax curves | C' (Kpa) | ϕ' (°) | K_0 | T_{max} |
| KSRH10 | 1 | 0-6 | 140 | 1520 | 0.49 | 1800 | 25 | 2 | 1 | 0 | 38 | 0.38 | [5-20] |
| | 2 | 6-11 | 180 | 1650 | 0.49 | 1800 | 25 | 2 | 2 | 0 | 38 | 0.38 | [20-30] |
| | 3 | 11-15 | 230 | 1650 | 0.49 | 1500 | 25 | 2 | 3 | 0 | 43 | 0.32 | [30-36] |
| | 4 | 15-20 | 300 | 1650 | 0.48 | 1500 | 25 | 2 | 3 | 0 | 43 | 0.32 | [36-43] |
| | 5 | 20-24 | 250 | 1650 | 0.49 | 1600 | 25 | 2 | 4 | 0 | 43 | 0.32 | [43-50] |
| | 6 | 24-28 | 370 | 1650 | 0.47 | 1600 | 25 | 2 | 5 | 0 | 38 | 0.38 | [50-58] |
| | 7 | 28-35 | 270 | 1650 | 0.49 | 1800 | 35 | 1.5 | 5 | 0 | 38 | 0.38 | [58-74] |
| | 8 | 35-39 | 460 | 1650 | 0.46 | 1800 | 25 | 2 | 6 | 259 | 16 | 0.72 | [74-57] |
| | 9 | 39-44 | 750 | 1800 | 0.48 | 2500 | 75 | 0.67 | - | - | - | - | - |
| | 10 | 44-84 | 1400 | 3400 | 0.44 | 2500 | 140 | 0.36 | - | - | - | - | - |
| | 11 | 84-255 | 2400 | 5900 | 0.35 | 2500 | 240 | 0.2 | - | - | - | - | - |
| SENDAI | 1 | 0-3 | EQ1 | EQ2 | 0.48 | 1850 | 20 | 0.025 | N°1-SENDAI | 0 | 44 | 0.31 | From 5 to 39 kPa |
| | 2 | 3-7 | | | 0.48 | 1890 | 25 | 0.020 | N°2-SENDAI | 0 | 44 | 0.31 | |
| | 3 | 7-8 | 550 | 2800 | 0.48 | 2480 | 55 | 0.009 | - | - | - | - | - |

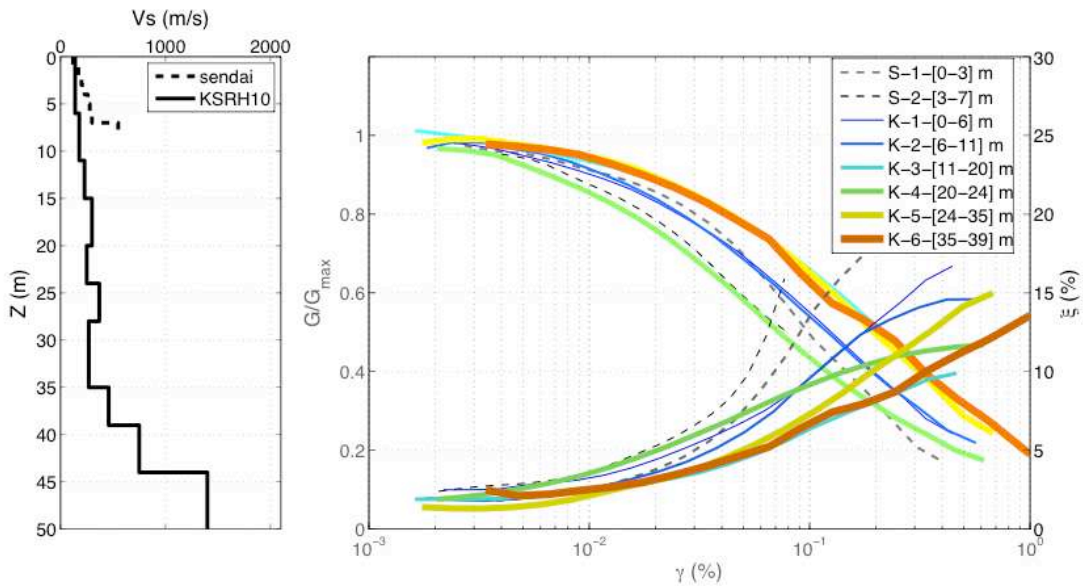


Figure 1: Vs profiles, G/Gmax and damping curves relative to shear strain, at Sendai and KSRH10 sites.

Input Motion Selection

The PGA and the frequency content of a recording are two relevant parameters of the input motion for describing the expected degree of non-linear soil behavior (Assimaki and Li, 2012). Nine input motions per site were selected, representing 3 different PGA levels (≥ 0.6 , 0.2-0.3 m/s² and ≤ 0.1 m/s² at the downhole sensor) and approximately 3 distinct frequency contents. PGA was calculated on the acceleration time histories as the quadratic mean of the EW and NS components, filtered between 0.1 and 40 Hz. The numbering of input motion corresponds to decreasing PGA level from #1 to #9.

The empirical borehole Fourier transfer functions (BFSR; here, the surface to downhole motion spectral ratio) is calculated for the 18 input motions, illustrated in Figure 2. For KSRH10, the inter-event BFSR variability is quite large as well as between components of a same event. This indicates that the site does not behave similarly from one component to another and may indicate a more complex site configuration than wished. At Sendai, we observe that the BFSR of the stronger motions 1 and 2 are shifted towards lower frequencies, while their amplitude is reduced compared to the other events, reflecting non-linear soil behavior during these events

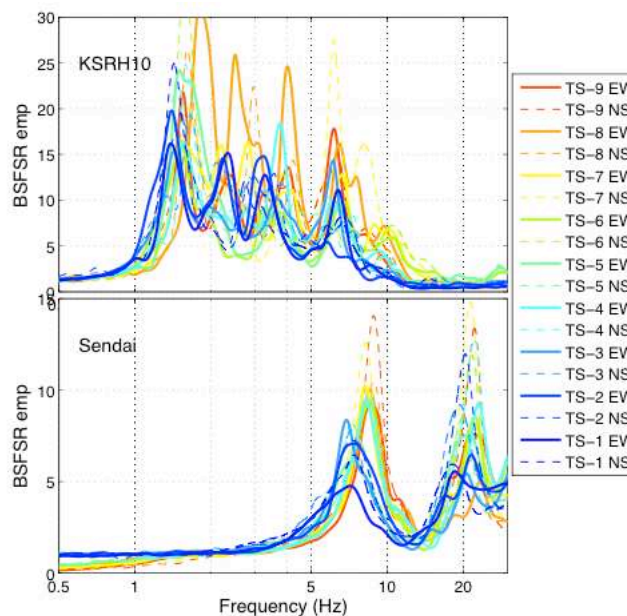


Figure 2: Comparison of the empirical transfer functions for the EW and NS components of each of the 9 input motions for sites KSRH10 (upper graph) and Sendai (lower graph).

Method of Analyses of the Computations

The 28 team/code couples were asked to calculate the propagation of 9 input motions at both sites. They had to provide, respectively, the accelerations for 8 and 12 virtual receiver locations (at the surface and interfaces) and the stress-strain histories at 7 and 11 locations (at the middle of each soil layer).

From these results, we then performed a comparative analysis for a number of parameters:

- a few engineering parameters as selected by (Anderson, 2004), i.e., PGA, response spectra at different period ranges, CAV, duration, and cross-correlation;
- surface / downhole sensor amplification for Fourier (BFSRs) and response spectra;
- depth dependence of peak shear strain, shear strength and PGA;
- G/Gmax curves, stress-strain curves at selected receivers; and
- additional time-frequency analyses (ratio between surface and downhole Stockwell-transforms).

Comparison of the Computations with Observations

For sake of conciseness, the comparison between the computed BFSRs and the observations is displayed here (Figure 3) only for the strongest (Input 1 for both sites) and one weak (Input 7 for both sites) input motions. The strongest input motion did indicates non-linear soil behavior has the corresponding site response was outside the average +/- one standard deviation of the site response computed for weak motions.

For the weak motion (Input 7), we can observe a general trend for an overestimation of the linear site response, which can be explained by: (1) inadequate soil properties parameterization such as overestimated soil quality factor (Q) values, (2) reference/downhole sensor location: it has been observed in many vertical arrays by comparing empirical weak motion and 1D linear visco-elastic numerical BFSRs, that destructive interferences between the up- and down-going waves at the downhole sensor are much higher in simulations (Regnier, 2013), due to oversimplified assumptions regarding the input motion incidence angle: the incident wavefield is certainly significantly different form a pure, vertically propagating, plane S-wave.

In addition, for KSRH10 only, at high frequencies (above 12 Hz), a de-amplification is observed in the empirical BFSR that is not reproduced by the simulations; it could be at least partially due to interactions between soil and instrument shelter for the surface sensor.

For the strongest input motion (input 1) at both sites, we observe that the non-linear soil behavior is under-estimated by most of the teams. Optionally, decreasing Q to reduce the weak motion discrepancy will also decrease deformation and consequently the non-linearity; therefore, we should revised either the non-linear soil parameters (to be more non-linear) or the type of analysis performed (total stress analysis).

- ⇒ The cyclic tri-axial lab measurements may suffer form uncertainties in revealing the non-linear soil behavior during earthquake shaking (different loading, water content and some disturbance of the sample...). Their interpretations can also a source of uncertainty, for instance regarding the conversion between axial and shear strains, or the value of the very low strain, elastic young modulus for the normalization.
- ⇒ The computations were performed with total stress analysis, so that some discrepancies could come from pore water pressure effects. One team (W) performed an effective stress

analysis and results show that, for Sendai, simulations are close to the observations, at least for the first resonance peak. Although it should be note that this team calibrated his non-linear soil model directly on the lab measurements and not the G/Gmax curves given by the organization.

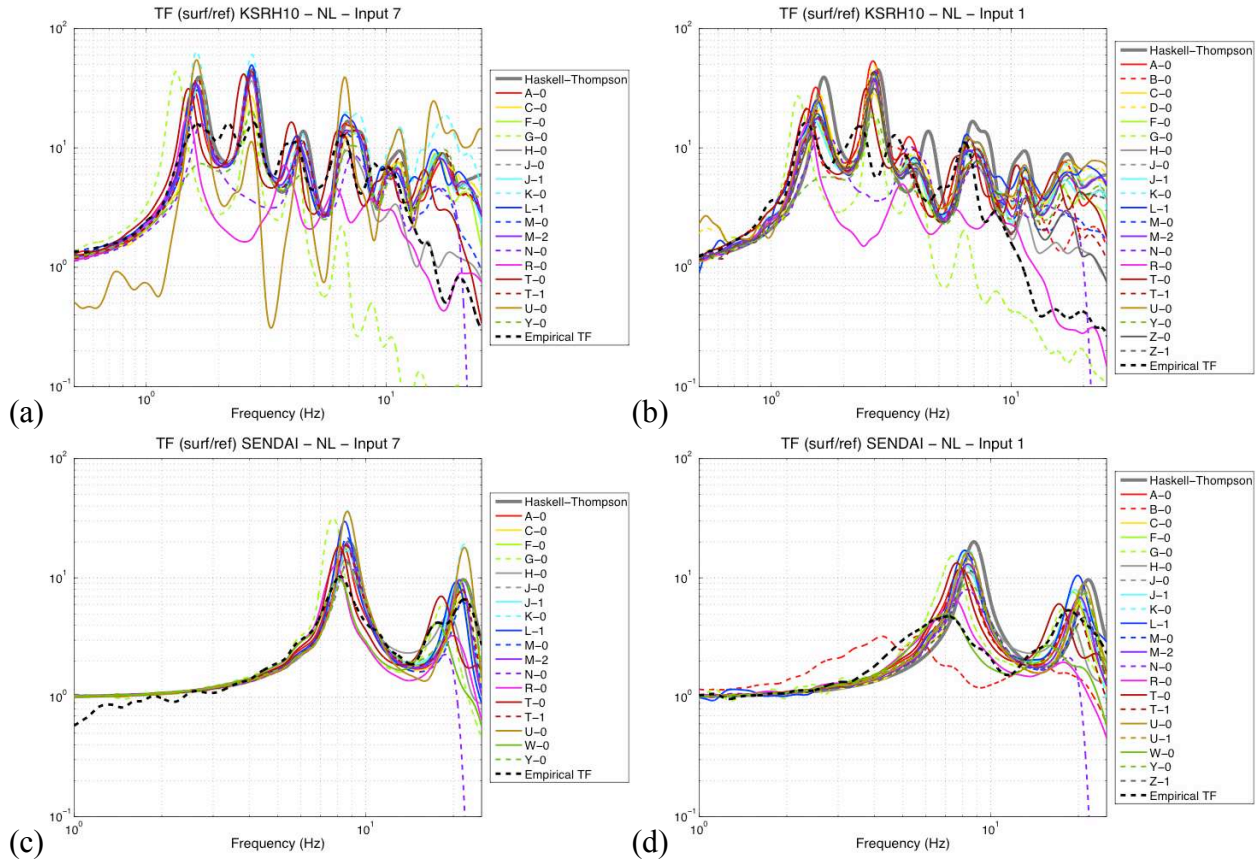


Figure 3: Borehole Fourier transfer functions for Inputs 7 (left panels) and 1 (right panels), for all computations, with respect to the Haskell-Thompson linear solution (grey curve) and to the empirical transfer function (black dotted line) for (a and b) KSRH10 and (c and d) Sendai.

To have an overview of the epistemic uncertainties, we calculated the average error between the empirical and computed surface response spectra for all events. The results are illustrated in Figure 4. Our initial expectations were that errors would be greater for the strongest input motions, as the non-linear soil effects are greater: this was observed in a preliminary verification phase comparing the results of different NL codes for increasing pga levels. However, no similar trend can be clearly observed here. We note that the results are very poor (large errors) for some inputs (**5** at Sendai, **5** and **8** at KSRH10), where they exceed 100% for short periods.

We explored into more detail these three input motions, using a particle motion analysis of the downhole recordings (filtered between 1-2Hz for KSRH10 and 7-10Hz for Sendai), and found that the considered EW-components are very weak compared to their NS-components, thus underestimating the total wavefield energy. In such cases, rotating the EW-component towards

the radial component, describing the highest shear wave energy, should improve the fitting of the earthquake surface recording. We should also note that the signal-to-noise ratio at low frequency for the weak motion records can be low.

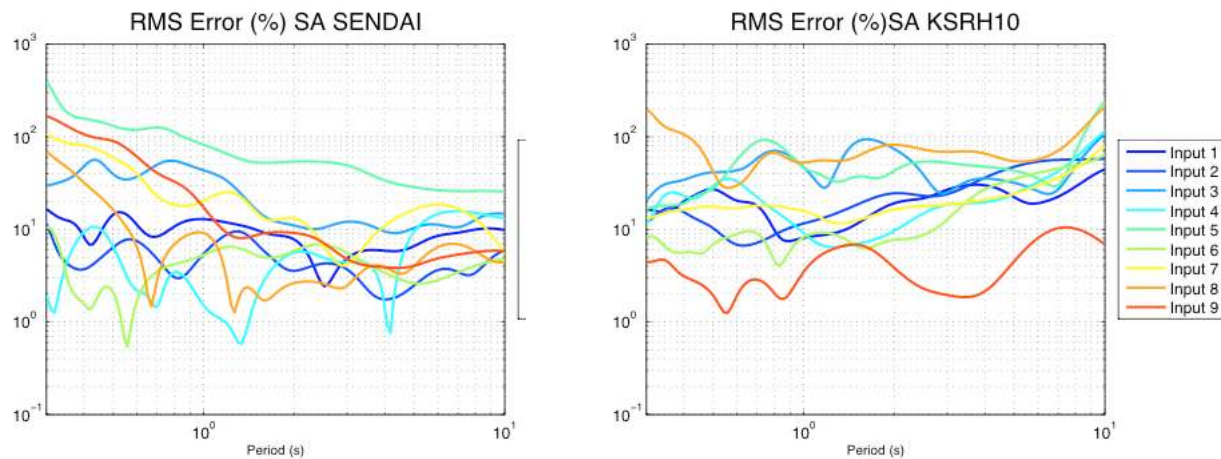


Figure 4: Root mean square error between the surface recordings and simulated pseudo-response spectra at Sendai (left figure) and KSRH10 (right figure).

Conclusions

This validation phase is still ongoing with a new iteration. However, the results of the first iteration very briefly reported here lead to two main conclusions regarding the surface / downhole amplifications on these data: (i) the simulated borehole transfer functions are always overestimated, and (ii) the amount of non-linearity is always underestimated. Such discrepancies can have several origins:

- uncertainties in the geotechnical and geophysical soil parameters used. They were however performed with state of the art tools.
- non-1D but rather 3D soil geometries. However, this issue was accounted for in the selection of sites, and such effects would have been worse at other sites.
- the consideration of only one component. This is however the common engineering practice for most of 1D NL site response studies.
- more complex, non-vertically propagating incident waves and more complex low strain attenuation with frequency dependency. Once again, this is however the basic assumption for most of usual engineering studies.

This first iteration was performed blindly for the whole set of input motions. Considering these first results, a second iteration with modified soil column and knowledge of the surface soil response is on-going with the objectives of (1) reducing the discrepancy between observations and computations, and (2) understanding the main sources of epistemic errors in the first iteration. The results of this second phase will be available before the end of 2015.

Acknowledgments

We acknowledge the dedicated and proactive participating teams from all over the world: D. Assimaki, J. Shi (Caltech, US), S. Iai (DPRI, Japan), S. Kramer (Univ. Washington, US) E. Foerster (CEA, France), C. Gelis & E. Delavaux (IRSN, France), A.Giannakou (Fugro, France), G. Gazetas E. Garini & N. Gerolymos (NTUA, Greece), J. Gingery (UCSD, US), Y. Hashash & J. Harmon (Univ. Illinois, US), P. Moczo, J.Kristek & A. Richterova (CUB, Slovakia), S. Foti & S. Kontoe (Politecnico di Torino & Imperial college, Italy) G. Lanzo (Univ. Roma La Sapienza, Italy) F. Lopez-Caballero & S. Montoya-Noguera (ECP, France), F. De-Martin (BRGM, France), B.Jeremic, F. Pisano & K. Watanabe (UCD, TU Delft & Shimizu Corp, US), A. Nieto-Ferro (EDF, France), A. Chiaradonna, F. Silvestri & G. Tropeano (UNICA, Italy), MP-Santisi d'Avila (UNS, Nice) D. Mercerat (CEREMA, France) and D. Boldini (UNIBO, Italie)

References

- Anderson, J.G.. Quantitative measure of the goodness-of-fit of synthetic seismograms. 13th World Conf. Earthq. Eng. 2004
- Assimaki, D., Li, W. Site and ground motion-dependent nonlinear effects in seismological model predictions. *Soil Dyn. Earthq. Eng.* 2012; 143–151.
- Kwok, A.O., Stewart, J.P., Hashash, Y.M. Nonlinear ground-response analysis of Turkey Flat shallow stiff-soil site to strong ground motion. *Bull. Seismol. Soc. Am.* 2008; **98**: 331–343.
- Regnier, J.. Variabilité de la réponse sismique: de la classification des sites au comportement non-linéaire des sols. Paris Est. 2013
- Stewart, J., Kwok, A. Nonlinear Seismic Ground Response Analysis: Protocols and Verification Against Array Data. *PEER Annu. Meet. San Franc.-Present.* 84. 2009.
- Thompson, E.M., Baise, L.G., Tanaka, Y., Kayen, R.E. A taxonomy of site response complexity. *Soil Dyn. Earthq. Eng.* 2012; **41**: 32–43.